Netherlands organization for applied scientific research

TNO-report

TNO Physics and Electronics Laboratory

P.O. Box 96864
2509 JG The Hague
Oude Waalsdorperweg 63
The Hague, The Netherlands

Fax +31 70 328 09 61
Phone +31 70 326 42 21

TD 91-3693

report no. FEL-91-A324

copy no. 8

title

High power millimetre-wave polarizers

AD-A256 558

author(s):

F.A. Nennie

date: April 1992

classification	
title	: unclassified
abstract	: unclassified
report text	: unclassified
appendices A and B	: unclassified

no. of copies	: 22
no. of pages	: 42 (incl. appendices, excl. RDP + distr. list)
appendices	: 2

All information which is classified according to Dutch regulations shall be treated by the recipient in the same way as classified information of corresponding value in his own country. No part of this information will be disclosed to any party.

92-28390

92 10 28 015

report no. : FEL-91-A324
title : High power millimetre-wave polarizers

author(s) : F.A. Nennie
institute : TNO Physics and Electronics Laboratory

date : April 1992
NDRO no. : A87KL064 and A85KLu126
no. in pow '91 : 710.5

Research supervised by:
Research carried out by:

ABSTRACT (UNCLASSIFIED)

The operation and realization of 4 high-power polarizers at 35.0 GHz and 94.0 GHz are described in this report.

Results of calculations and measurements are discussed.

The realized polarizers make use of an elliptical waveguide to convert the linearly polarized incident wave into an outward left or right-hand circularly polarized wave.

Main measurement results are:

The axial ratio at 35.0 GHz is less than 1.0 dB over 5 percent bandwidth. The return loss is better than 21 dB (VSWR < 1.2) over more than 30 percent bandwidth. The insertion loss is less than 0.3 dB over more than 30 percent bandwidth. The isolation is more than 18 dB over 5 percent bandwidth. The maximum peak-power is 63 kW.

The axial ratio at 94.0 GHz is less than 1.0 dB over 5 percent bandwidth. The return loss is better than 26 dB (VSWR < 1.1) over more than 3 percent bandwidth. The insertion loss is less than 0.75 dB over more than 3 percent bandwidth. The isolation is more than 20 dB over 3 percent bandwidth. The maximum peak-power is 9.5 kW.

All polarizers have been made waterproof and dust-proof.

rapport no.	:	FEL-91-A324
titel	:	Hoog vermogen millimetergolf polarisatoren
auteur(s)	:	F.A. Nennie
instituut	:	Fysisch en Elektronisch Laboratorium TNO
datum	:	april 1992
hdo-opdr.no.	:	A87KL064 en A85KLu126
no. in iwp '91	:	710.5
Onderzoek uitgevoerd o.l.v.	:	
Onderzoek uitgevoerd door	:	

SAMENVATTING (ONGERUBRICEERD)

Dit rapport geeft een beschrijving van de werking en realisatie van 4 hoogvermogen polarisatoren op 35.0 GHz en 94.0 GHz.
De resultaten van berekeningen en metingen worden besproken.
De gerealiseerde polarisatoren maken gebruik van een elliptische golfpijp om de lineair gepolariseerde inkomende golf om te zetten in een uitgaande links of rechts draaiende circulair gepolariseerde golf.
De belangrijkste meetresultaten zijn:
De ellipticiteit van de polarisatie op 35.0 GHz is minder dan 1.0 dB over 5 procent bandbreedte. De reflectie verliezen zijn beter dan 21 dB over meer dan 30 procent bandbreedte. De transmissie verliezen zijn minder dan 0.3 dB over meer dan 30 procent bandbreedte. De isolatie is meer dan 18 dB over 5 procent bandbreedte. Het maximaal vermogen is 63 kW.
De ellipticiteit van de polarisatie op 94.0 GHz is minder dan 1.0 dB over 5 procent bandbreedte. De reflectie verliezen zijn beter dan 26 dB over meer dan 3 procent bandbreedte. De transmissie verliezen zijn minder dan 0.75 dB over meer dan 3 procent bandbreedte. De isolatie is meer dan 20 dB over 3 procent bandbreedte. Het maximaal vermogen is 9.5 kW.
Alle polarisatoren zijn waterdicht en stofdicht gemaakt.

CONTENTS

ABSTRACT		2
SAMENVATTING		3
CONTENTS		4
1.0	INTRODUCTION	6
2.0	PRINCIPLE OF OPERATION	7
2.1	Polarization	8
2.2	Tolerance calculations	11
3.0	POLARIZER PARTS	18
3.1	Chokes	20
4.0	POLARIZER MEASUREMENTS	21
4.1	Axial ratio measurements	21
4.2	35.0 GHz network analyser measurements	22
4.3	94.0 GHz network analyser measurements	27
5.0	CONCLUSION	32
6.0	NOMENCLATURE	33
7.0	BIBLIOGRAPHY	34

APPENDIX A: A DERIVATION OF THE EQUATION OF THE PHASE SHIFT IN AN ELLIPTICAL WAVEGUIDE

APPENDIX B: AN APPROXIMATION OF THE CUT-OFF FREQUENCY OF AN ELLIPTICAL WAVEGUIDE

1.0 INTRODUCTION

For radar reflection measurements radarsystems at 35 and 94 GHz have been built at TNO Physics and Electronics Laboratory.

Among the components being used in these radarsystems are high power polarizers (above 25 kW at 35 GHz and above 1.5 kW at 94 GHz).

Commercially available polarizers are offered by corporations as Millitech, Alpha Ind. and Hughes. The conversion of the linear polarized signal in a circular waveguide (operating in the dominant TE_{11} mode) to a circularly polarized signal has been accomplished by using a dielectric 'quarter-wave' plate.

The maximum peak power of these commercially polarizers is 5 kW at 35 GHz and 1 kW at 94 GHz.

Since 'quarter-wave' plate polarizers do not meet the high power requirements, a high power elliptical waveguide polarizer has been developed at TNO Physics and Electronics Laboratory.

In this report we will discuss the principles and development of the elliptical waveguide polarizer.

In chapter 2.0 we will discuss the basic theory of the elliptical polarizer.

The waveguide, tapers and choke parts are described in chapter 3.0 and 3.1, whereas chapter 4.0 gives information on the measurements.

The conclusions can be found in chapter 5.0.

Appendix A gives the derivation of the equation of the phase shift in the elliptical waveguide using the cut-off wavelength of circular waveguides.

Appendix B gives an approximation of the cut-off frequency of an elliptical waveguide.

This work has been carried out under assignment number A87KL064 and A85KLu126.

2.0 PRINCIPLE OF OPERATION

A linearly polarized wave (E_r) can be resolved into two orthogonal linearly polarized components of equal amplitude (e_θ and e_ϕ). We assume that the elliptical waveguide can be decomposed into two different circular waveguides.This is illustrated in figure 2.0.0.

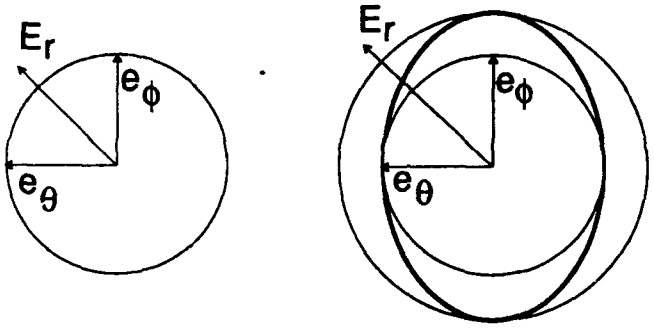

Fig. 2.0.0: Schematic representation of the elliptical polarizer using a double circular waveguide model.

Each of the orthogonal components e_θ and e_ϕ behave as if they were propagating in one of the two circular waveguides (in TE_{11}-mode).

Since the waveguide wavelengths λ_g of the circular waveguides are different, a phase shift ψ between both orthogonal components will result which is proportional to the axial length of the waveguide.

When the axial length and cross section of the elliptical waveguide are chosen appropriately, a 90° phase difference between the orthogonal components e_θ and e_ϕ can be achieved and the linearly polarized wave is converted into a circular polarized wave. Figure 2.0.1 shows this conversion.

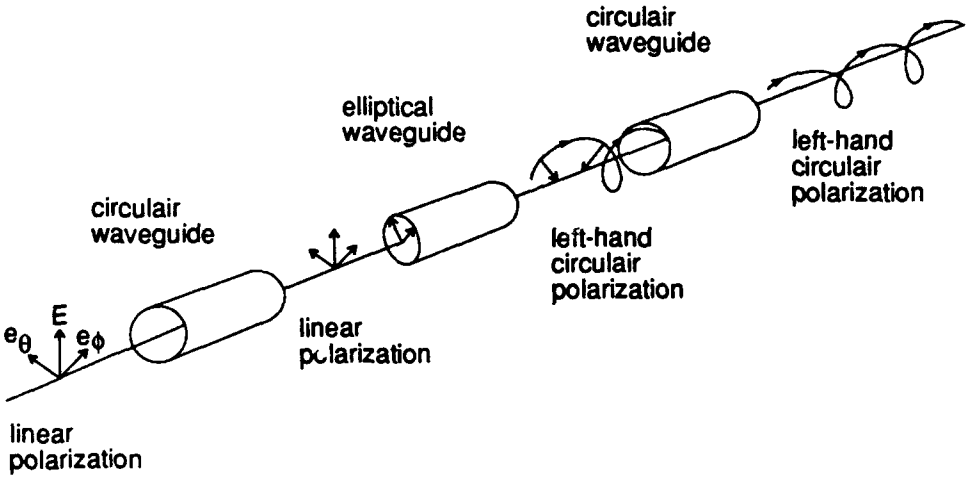

Fig. 2.0.1: Conversion from linear to circular polarization.

The definition of polarization is :
To an observer looking in the direction of propagation, a counter-clockwise rotating electric field in a cross section is called left-hand circular polarized (L.C.P.).[5]

2.1 Polarization

The two orthogonal linearly polarized components can be expressed using a cosine function to represent the sinusoidal variation of the field as a function in time.

$$e_\theta = E_1 \cos \omega t \text{ and } e_\phi = E_2 \cos(\omega t + \psi) \qquad (1)$$

E_1 and E_2 are the amplitudes of the two orthogonal components, ψ represents the phase shift between those components and ω is the radial frequency.
In order to find the sense of rotation of the resulting field vector at a fixed point in space, the time factor has to be eliminated.
Substitution of the expression for e_θ in that for e_ϕ gives, after some mathematical manipulations :

$$\left(\frac{e_\theta}{E_1}\right)^2 + \left(\frac{e_\phi}{E_2}\right)^2 - \frac{2\,e_\theta e_\phi}{E_1 E_2}\cos\psi = \sin^2\psi \qquad (2)$$

This is the equation of an ellipse. Actually, all polarizations can be considered elliptical, since the circular and linear polarizations are special cases of the polarization ellipse. So, it is interesting to consider the special cases to gain an understanding of the relationships between the orthogonal components for different polarizations.

case a: $E_1 = E_2 = E$ and $\psi = +90°$.

$$\left(\frac{e_\theta}{E}\right)^2 + \left(\frac{e_\phi}{E}\right)^2 = 1 \qquad (3)$$

This is the equation of a circle and since $\psi = +90°$;

$e_\theta = E\cos\omega t$ and $e_\phi = -E\sin\omega t$.

The resulting field vector rotates clockwise for an observer looking in the direction of propagation and is called right-hand circular polarization.

case b: $E_1 = E_2 = E$ and $\psi = -90°$.

$$\left(\frac{e_\theta}{E}\right)^2 + \left(\frac{e_\phi}{E}\right)^2 = 1 \qquad (4)$$

This is the equation of a circle and since $\psi = -90°$;

$e_\theta = E\cos\omega t$ and $e_\phi = E\sin\omega t$.

The resulting field vector rotates counter-clockwise for an observer looking in the direction of propagation and is called left-hand circular polarization.

case c: $E_1 \neq E_2$ and $\psi = 0°$.

$$\frac{e_\theta}{E_1} - \frac{e_\phi}{E_2} = 0 \qquad (5)$$

This is the equation of a straight line and we are dealing with an arbitrary linear polarization. The resulting field vector makes an angle τ with the E_1 field vector and is given by the equation;

$$\text{angle } (\tau) = \arctan(E_2/E_1) \qquad (6)$$

case d: $E_1 = E_2 = E$ and $\psi = 0^\circ$.

$$\frac{e_\theta}{E_1} - \frac{e_\phi}{E_2} = 0 \qquad (7)$$

This is the equation of a straight line and we are dealing with linear polarization. The angle $\tau = 45^\circ$.

case e: $E_1 \neq E_2$ and $\psi = \pm 90^\circ$.

$$\left(\frac{e_\theta}{E_1}\right)^2 + \left(\frac{e_\phi}{E_2}\right)^2 = 1 \qquad (8)$$

This is the equation of an ellipse and we are dealing with elliptical polarization. The major-axis and minor-axis of the ellipse are parallel to the electric field vectors. The $\pm$ sign is related to the rotation sense of the resulting field vector in the same way as explained in case a and b.

case f: $E_1 \neq E_2$ and $\psi \neq n * 90^\circ$ (n = integer).

$$\left(\frac{e_\theta}{E_1}\right)^2 + \left(\frac{e_\phi}{E_2}\right)^2 - \frac{2e_\theta e_\phi}{E_1 E_2} \cos\psi = \sin^2\psi \qquad (9)$$

This is the equation of an ellipse and we call it arbitrary elliptical polarization. The major-axis makes an angle τ with the E_1 field vector and can be calculated with (6). The $\pm$ sign is related to the sense of the e-vector in the same way as explained in case a.

case g: $E_1 = E_2 = E$ and $\psi \neq n * 90^\circ$ (n = integer).

$$\left(\frac{e_\theta}{E}\right)^2+\left(\frac{e_\phi}{E}\right)^2-\frac{2e_\theta e_\phi}{E^2}\cos\psi = \sin^2\psi \qquad (10)$$

This is the equation of an ellipse and we call it elliptical polarization. The major-axis and minor-axis of the ellipse are parallel to the electric field vectors. The ± sign is related to the sense of the e-vector in the same way as explained in case a.

2.2 Tolerance calculations

In chapter 2.1 we described the importance of an exact 90 degrees phase shift in the elliptical part of the polarizer. Figure 2.2.0-A shows the inside waveguide of the polarizer.

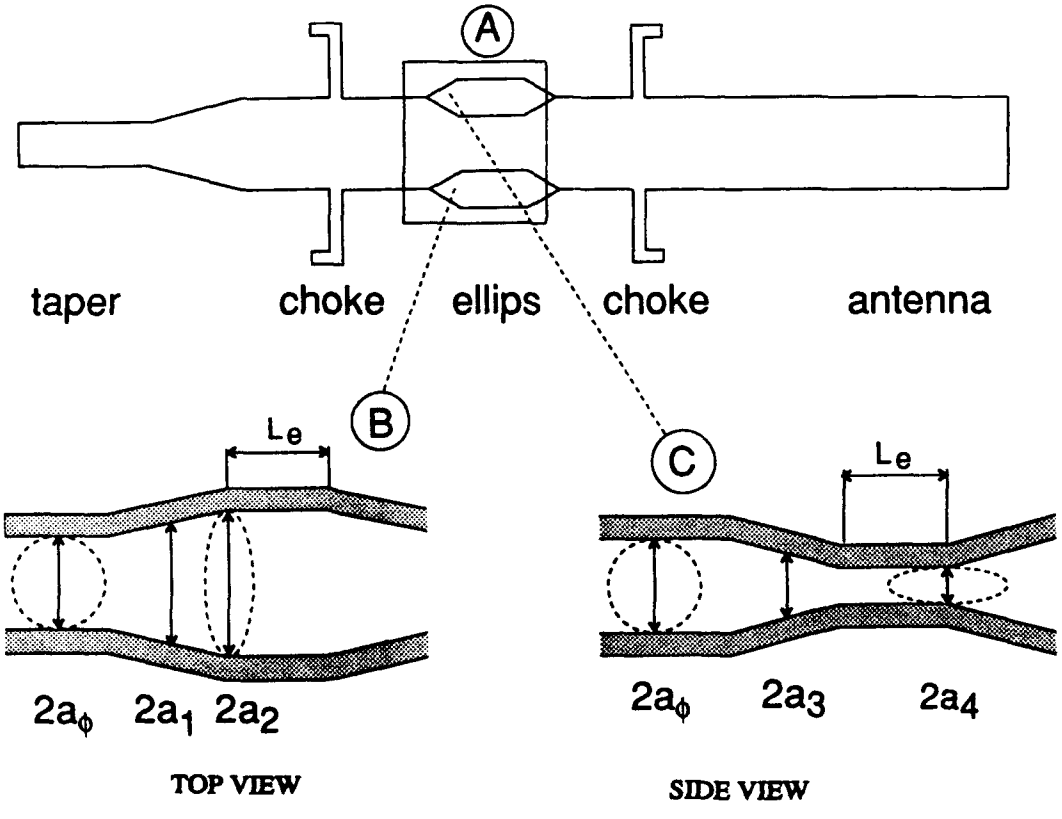

Fig. 2.2.0: Inside dimensions of the polarizer.

In figures 2.2.0-B and 2.2.0-C the centre part is enlarged. The standard circular inside waveguide-diameter $2a_0$ is 6.35 mm for 35.0 GHz (WR-28) and 2.39 mm for 94.0 GHz (WR-10).

After deforming the circular waveguide over a length L_e, the broad inside waveguide-diameter is $2a_2$ and the narrow inside waveguide-diameter is $2a_4$.
These are illustrated in figure 2.2.1. Figure 2.2.2 also shows the deformed waveguide.

Fig. 2.2.1: The elliptical waveguide (35.0 GHz).

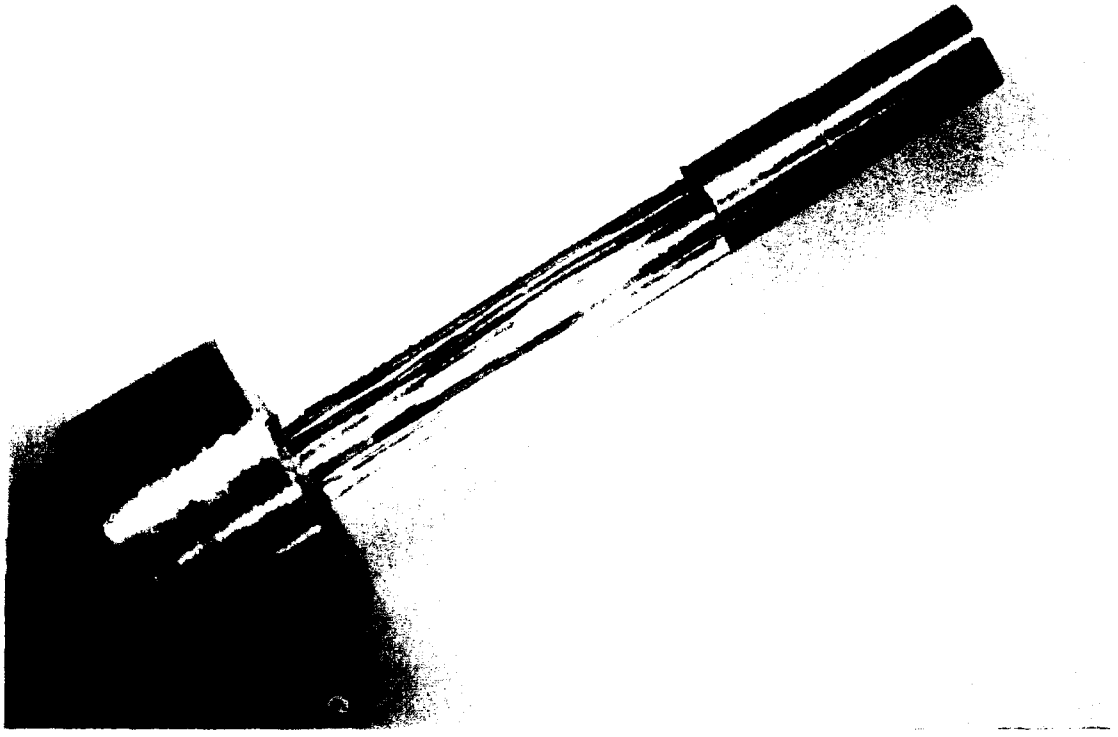

Fig. 2.2.2: Over a length of 5.6 mm the waveguide is deformed (94.0 GHz).

The phase shift in the elliptical section can be approximated with the aid of the following equation;

$$\psi_e = 360 L_e \left(\frac{\sqrt{1-(\lambda_0/3.412\, a_2)^2} - \sqrt{1-(\lambda_0/3.412\, a_4)^2}}{\lambda_0} \right) \qquad (11)$$

Here λ_0 is the free space wavelength and L_e is the length of the non-tapered elliptical waveguide section.

In appendix A the derivation of this equation is described.

Figure 2.2.3 A + B show the waveguide wavelength λ_g as a function of the width of the circular waveguide in which the TE_{11} mode propagates. In the tapered section the diameter of the waveguide changes from $2a_0$ to $2a_2$ and from $2a_0$ to $2a_4$.

We used the average value of 2a for calculating the phase shift of the tapered section ($a_3 = (a_4+a_0)/2$ and $a_1 = (a_2+a_0)/2$).

So the use of these values a_1 and a_3 in equation (11) gives the phase shift ψ_t in the tapered section.

The length L_t is the total length of the two tapered elliptical waveguides and is calculated as follows :

$$L_t = \frac{(a_0-a_4)+(a_2-a_0)}{\tan \alpha} \qquad (12)$$

Where α is the angle of the taper.

The total polarizer phase shift ψ_p is :

$$\psi_p = \frac{360\left(L_e\left(\sqrt{1-\left(\frac{\lambda_o}{3.41a2}\right)^2} - \sqrt{1-\left(\frac{\lambda_o}{3.41a4}\right)^2} \right) + L_t\left(\sqrt{1-\left(\frac{\lambda_o}{3.41a1}\right)^2} - \sqrt{1-\left(\frac{\lambda_o}{3.41a3}\right)^2} \right) \right)}{\lambda_o} \qquad (13)$$

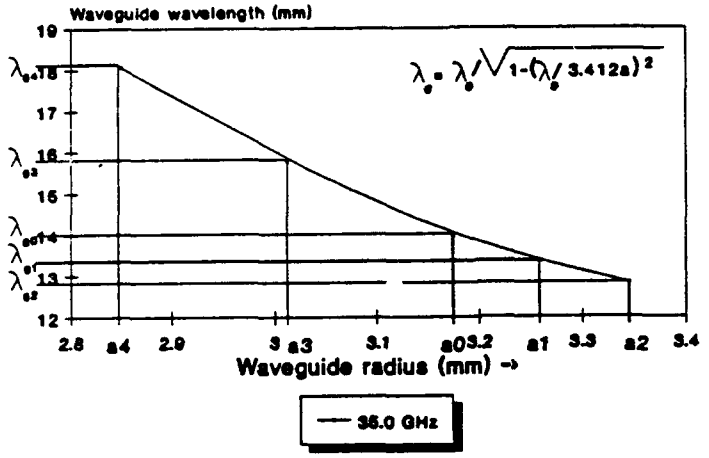

Fig. 2.2.3-A: The circular waveguide wavelength as a function of the waveguide-radius at 35.0 GHz.

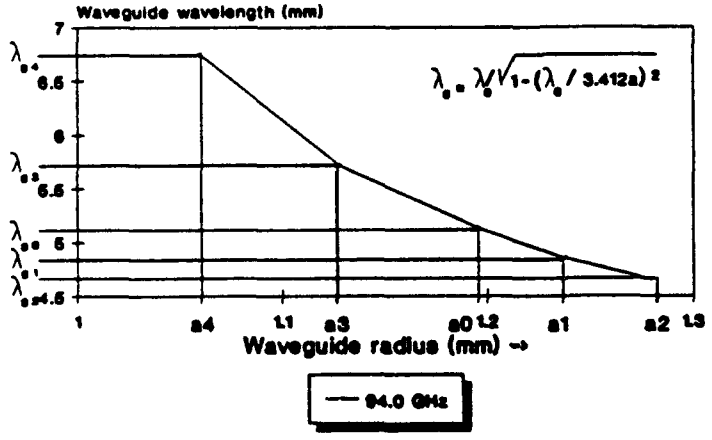

Fig. 2.2.3-B: The circular waveguide wavelength as a function of the waveguide-radius at 94.0 GHz.

	Polarizer 3			Polarizer 2			Polarizer C			Polarizer B		
	α = 2.7 deg. L_t = 10.49 mm L_e = 4.0 mm a0 = 3.175 mm a1 = 3.26 mm a2 = 3.345 mm a3 = 3.0125 mm a4 = 2.85 mm λ_0 34 = 8.817 mm λ_0 35 = 8.565 mm λ_0 36 = 8.337 mm			α = 2.7 deg. L_t = 11.98 mm L_e = 4.0 mm a0 = 3.175 mm a1 = 3.2725 mm a2 = 3.37 mm a3 = 2.99 mm a4 = 2.805 mm λ_0 34 = 8.817 mm λ_0 35 = 8.565 mm λ_0 36 = 8.337 mm			α = 2.7 deg. L_t = 4.66 mm L_e = 1.8 mm a0 = 1.195 mm a1 = 1.2375 mm a2 = 1.28 mm a3 = 1.1275 mm a4 = 1.06 mm λ_0 93 = 3.224 mm λ_0 94 = 3.189 mm λ_0 95 = 3.156 mm			α = 2.7 deg. L_t = 4.98 mm L_e = 1.8 mm a0 = 1.195 mm a1 = 1.24 mm a2 = 1.285 mm a3 = 1.1225 mm a4 = 1.05 mm λ_0 93 = 3.224 mm λ_0 94 = 3.189 mm λ_0 95 = 3.156 mm		
	34.0	35.0 (GHz)	36.0	34.0	35.0 (GHz)	36.0	93.0	94.0 (GHz)	95.0	93.0	94.0 (GHz)	95.0
ψ_e (deg)	34.8	31.5	29.0	41.3	37.2	34.1	44.6	43.1	41.5	47.8	46.0	44.8
ψ_t (deg)	39.7	37.6	34.9	54.1	49.5	45.9	52.0	50.8	48.9	59.8	58.0	56.5
ψ_p (deg)	74.5	69.1	63.9	95.4	86.7	80.0	96.6	93.9	90.4	108	104	101
Frequency for which ψ_p = 90 degr.	31.1 (GHz)			34.7 (GHz)			95.1 (GHz)			98.1 (GHz)		

Table 1: Some calculated polarizer data.

For each polarizer, calculations have been done at 3 frequencies with a 1 GHz interval. The results are summarized in table 1. It shows that at 35.0 GHz the calculated phase shift was 20.9° respectively 3.3° below 90°. At 94.0 GHz the calculated phase shift was 3.9° respectively 14° above 90°.

The phase shift is frequency dependent. For the 35.0 GHz polarizers this is 7.5°/GHz and for the 94.0 GHz ones this is 3°/GHz.

Changing the narrow inside elliptical waveguide-radius by 10μm results in a differential phase shift at 35.0 GHz of 3.9° and at 94.0 GHz of 10.1°.

In practice, we used equation (13) to get an approximation of the inside dimensions of the elliptical waveguide. Then we deformed the circular waveguide carefully and we measured the axial ratio of the polarizer.

Finally, to get an exact 90° phase shift we deformed the waveguide some extra μmeters.

Reducing the narrow waveguide radius 130 μm at 94.0 GHz gives a 90° phase shift. Reducing an extra 113 μm gives a total phase shift of 270°. When a pressing error has been made and the phase shift is 270°, the polarizer will work in the opposite circular direction.

In table 2 the narrow inside elliptical waveguide-radius, the maximum peak-power and the cut-off frequency are calculated for a phase shift of 0°, 90° and 270°.

94.0 GHz				35.0 GHz			
a_4	Ψ_p	Pmax	f_c	a_4	Ψ_p	Pmax	f_c
(mm)	(°)	(kW)	(GHz)	(mm)	(°)	(kW)	(GHz)
1.195	0	21.4	73.5	3.175	0	111	27.7
1.065	90	9.5	82.5	2.795	90	63	31.5
0.952	270	3.0	92.3	2.540	270	20	34.6

Table 2: The narrow inside elliptical waveguide-radius, the maximum peak-power and the cut-off frequency are calculated for a phase shift of 0°, 90° and 270°.

For a circular waveguide operating in the dominant or TE_{11} mode the maximum power is:

$$P_{max} = 450000\, d^2 \lambda_0 / \lambda_g \ \text{(W) [4]} \qquad (14)$$

Where d is the diameter of the circular waveguide in centimetres and λ_g is the circular waveguide wavelength in centimetres.
When the phase shift is 270°, the narrow waveguide size a_4 at 35.0 GHz is 2.54 mm and the waveguide wavelength is 48.7 mm. Using these parameters in (14) gives a maximum power of 20.1 kW which is 5 dB under the peak power level of a polarizer with a 90°phase shift.
The reduction of the narrow waveguide size also decreases the cut-off wavelength (λ_c). For the circular TE_{11} mode this wavelength is:

$$\lambda_c = 3.412\, a_4 \qquad (15)$$

When the centre frequency is 35.0 GHz and a_4 is 2.54 mm, the cut-off frequency (f_c) is 34.6 GHz. A small waveguide reduction of only 30 μm will cause a f_c higher than 35.0 GHz. When the centre frequency is 94.0 GHz and a_4 is 0.952 mm, f_c is 92.3 GHz and this allows an irregularity of 17 μm. This explains why we exercised the greatest care during the deforming procedure.

3.0 POLARIZER PARTS

Figure 3.0.0 shows a 35.0 GHz polarizer and figure 3.0.1 shows a 94.0 GHz polarizer.Rotating the black outer cylinder, of the polarizer, will change the sense of polarization. LC stands for left-hand circular, RC for right-hand circular and LIN for linear polarization.

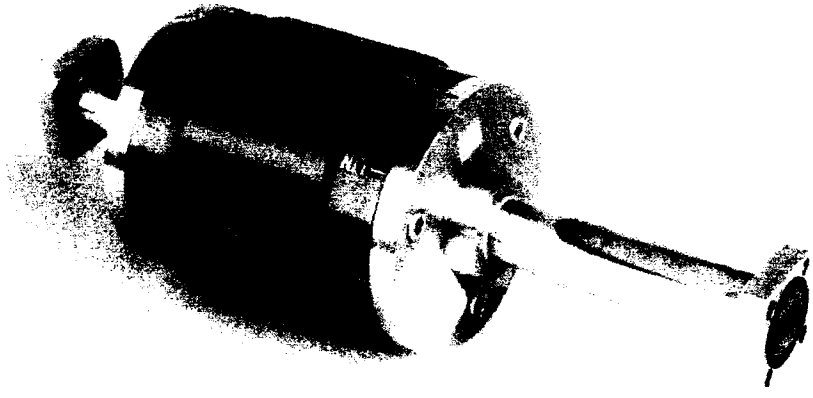

Fig. 3.0.0: 35.0 GHz polarizer.

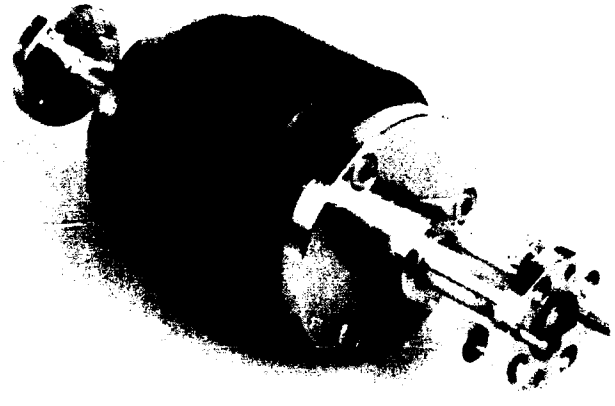

Fig. 3.0.1: 94.0 GHz polarizer.

Figures 3.0.2 and 3.0.3 show the test-polarizer.

Fig. 3.0.2: 35.0 GHz test-polarizer.

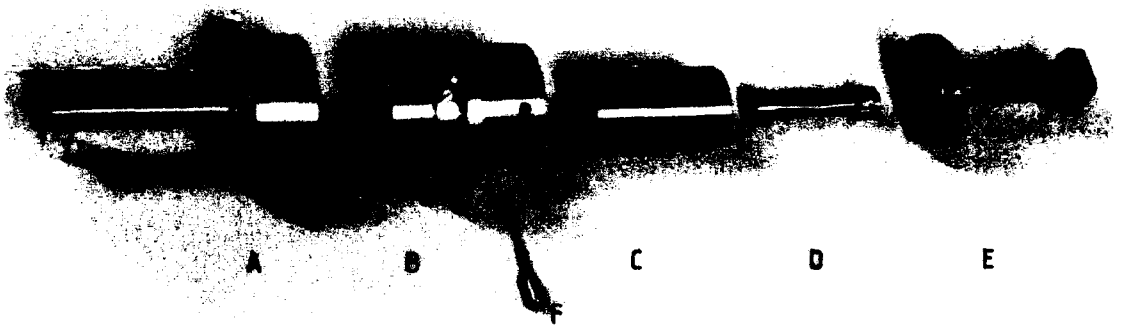

Fig. 3.0.3: Test polarizer parts.

In the test-polarizer the black outer cylinder is replaced by a metal bar (part F), with which the inner cylinder can be rotated over 90°. Part B is a non-movable part on which the tapers are screwed. In this cylinder some holes are made through which the adjustment screws pass.
The metal bar fits in a hole in part C. The screws in part C are used to adjust the inner cylinder D exactly in the linear polarization position. The inner cylinder is deformed in the middle. Part E is the tapering section in which the rectangular waveguide mode TE_{10} is converted into the TE_{11} mode. There are chokes between the taper part and antenna part. These chokes allow good impedance matching despite lack of good mechanical matching. For axial-ratio measurements we used a second taper instead of the antenna part. In this second taper a horizontal vane-load was installed.
In chapter 3.1 we discuss the chokes briefly.

3.1 Chokes

Parts C and D can rotate with respect to part E, in order to change the sense of polarization. To ensure good electrical connection between part E and parts C and D, we used a choke joint. This is illustrated in figure 3.1.0.

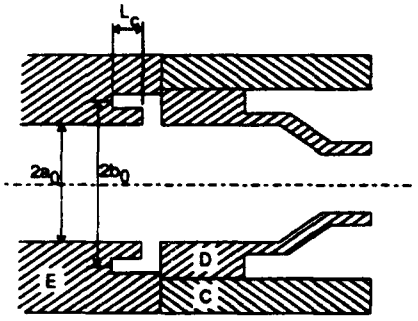

Fig. 3.1.0: Polarizer choke.

Freq.	(GHz)	35.0	94.0
L_c	(mm)	2.300	0.826
b_0	(mm)	5.217	1.958
a_0	(mm)	3.175	1.195

Table 3: Choke sizes.

The choke flange has a circular slot which is actually a short-circuited line, a quarter-wavelength long (L_c). This slot is also at a quarter-wavelength distance from the circular waveguide ($(2b_0-2a_0)/2$) and is an open circuit or infinite impedance.

The choke sizes were calculated with the aid of the information given in [1] and are presented in table 3.

4.0 POLARIZER MEASUREMENTS

Preliminary measurements of the polarizer-tools (circular load, horizontal vane-load, choke ring, waveguide 'rotary-joint' and circular antenna part) have been done but are not described in this report.
Only the measurements of the final polarizers are given.
In chapter 4.1 the measurements of the axial ratio and in chapter 4.2 the insertion loss, return loss and isolation are given.

4.1 Axial ratio measurements

The axial ratio measurements have been performed with the aid of a HP8755A Swept Amplitude Analyser (35.0 GHz) and a Hughes 47326H broadband detector receiver (94.0 GHz).
The axial ratio of the electrical field in the inner cylinders (part D in figure 3.0.4) was measured in the test-polarizer. The antenna piece of part A was replaced by a second taper (like part E), which could rotate over 360° in the large cylinder of part A. In order to prevent reflections of the cross polar component, we installed a horizontal vane-load in the circular waveguide part of the taper. The insertion loss of the horizontal vane-load is 0.5 dB for 35.0 GHz and 0.6 dB for 94.0 GHz.
Figure 4.1.0 gives the axial ratio of the circular polarized wave as a function of the frequency. The axial ratio is better than 1 dB over 5 percent frequency bandwidth for 35.0 GHz and 94.0 GHz.

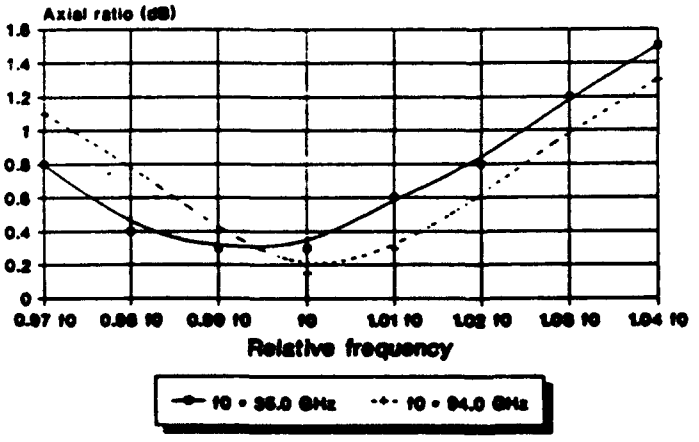

Fig. 4.1.0: The axial ratio of the circular polarized wave as a function of the frequency. The taper is rotated over 360°.

4.2 35.0 GHz network analyser measurements

The 35.0 GHz measurements were performed with the aid of a HP8510A Network Analyser with a HP8514A S-parameter test-set.

Polarizers number 2 and 3 were connected back to back to each other. The circular antenna-flanges were joined. In this way no horizontal vane-load was necessary and the measured insertion loss was the actual loss of both polarizers.

The return loss (S_{11}) of this polarizer combination is presented in figure 4.2.0 for linear and both circular polarizations and is better than 21 dB over 30 percent frequency bandwidth.

Figure 4.2.1 shows the insertion loss (S_{21}) for linear and both circular polarizations. The insertion loss of this polarizer combination is 0.6 dB over a 30 percent frequency bandwidth.

In figure 4.2.2 the isolation (S_{21}) for both circular polarizations is given. The isolation is more than 18 dB over a 5 percent frequency bandwidth.

We also measured the time domain response of polarizer 3. The circular antenna part was open. The time domain response is shown in 4.2.3A and 4.2.3C. The return loss is presented in figures 4.2.3B and 4.2.3D.

The frequency span is 6 GHz and the number of measurements-points is 401.

The response resolution is the minimum spacing between two equal responses with which they are identifiable. The minimum response resolution should be 1.96/frequency span [6] and is 320 psec assuming that we are dealing with band-pass impulses.

The longest delay that can be measured without ambiguity is the alias free range and can be calculated as follows:

$$\text{Alias free range} = \frac{\text{Resolution} * (\text{points}-1)}{1.96} = 20.8 \text{ nsec} \qquad (16)$$

Figure 4.2.3A shows two major discontinuities. The first one is due to the waveguide-taper and the second one is due to the open circular waveguide. There are three minor discontinuities: the rectangular waveguide-flange, the first choke and the second choke.

The distance between the second choke and the open circular waveguide is 180 psec and the response of the open waveguide is much larger than that of the second choke, so they begin to overlap (masking).

The response of the rectangular flange and the open circular waveguide has been removed in figure 4.2.3C with gating. The gate-start is placed after the rectangular waveguide-flange and before the waveguide-taper. The gate-stop is placed after the second choke and before the open circular waveguide.

Transforming back to the frequency domain the result is the return loss of polarizer 3 alone (figure 4.2.3D).

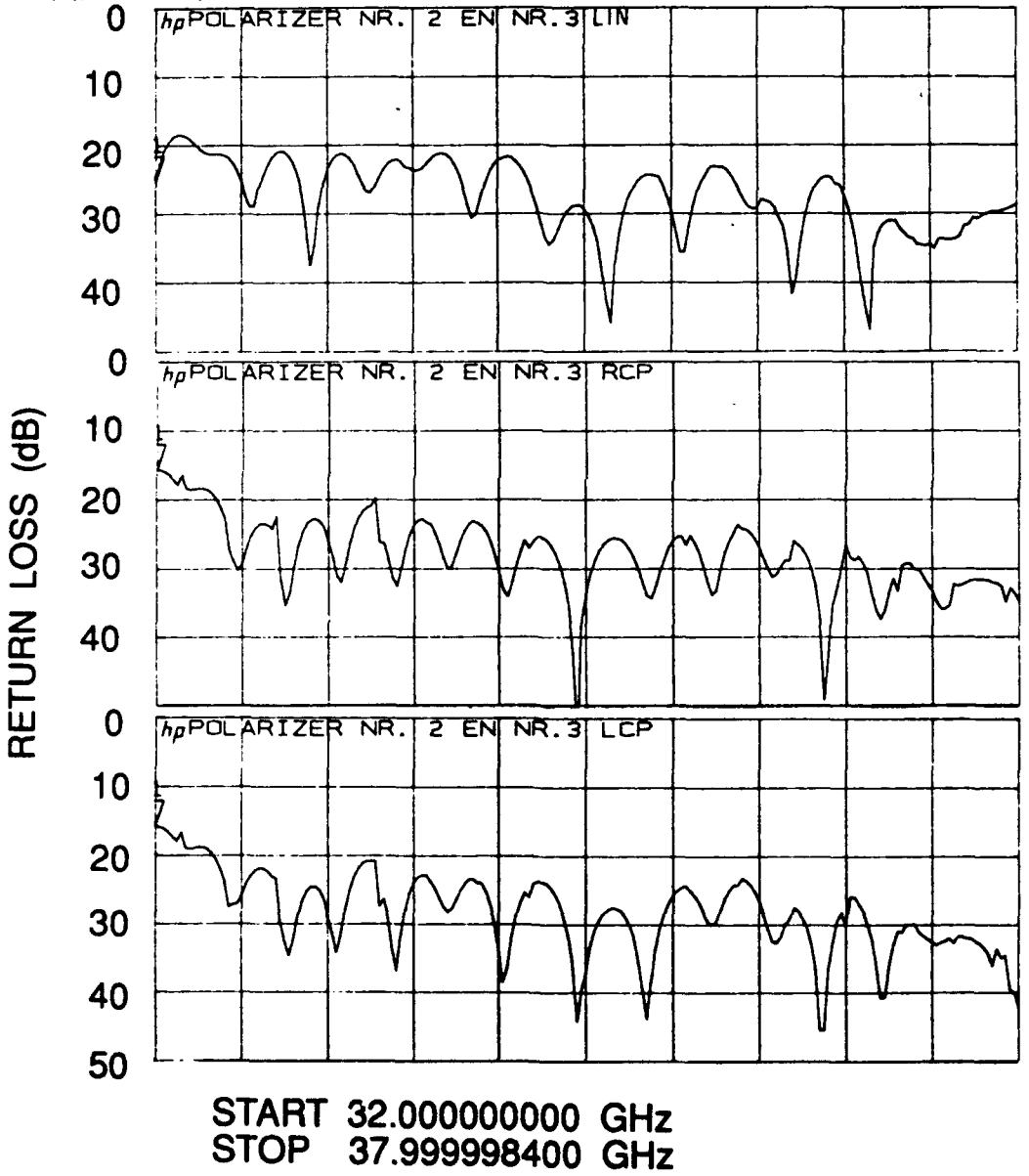

Fig. 4.2.0: The return loss of the polarizer combination 2 and 3 as a function of the frequency for linear, right-hand circular and left-hand circular polarization.

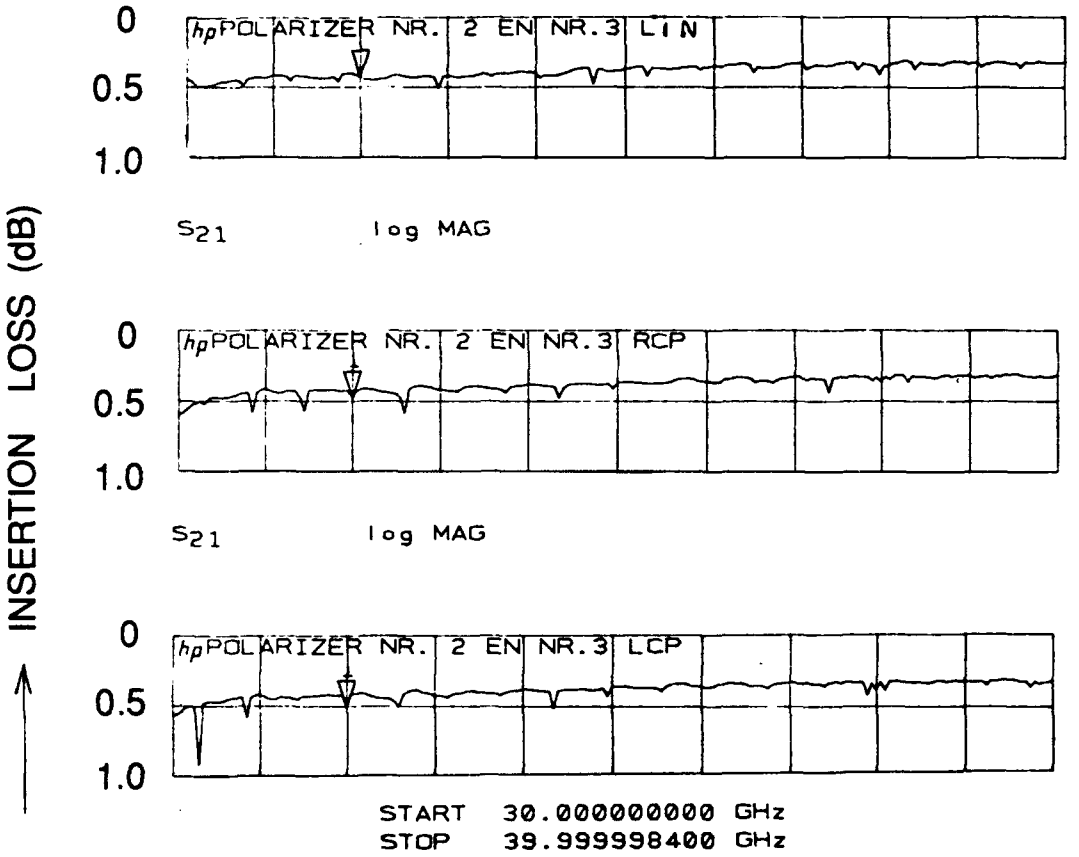

Fig. 4.2.1: **The insertion loss of the polarizer-combination 2 and 3 as a function of the frequency for linear, right-hand circular and left-hand circular polarization.**

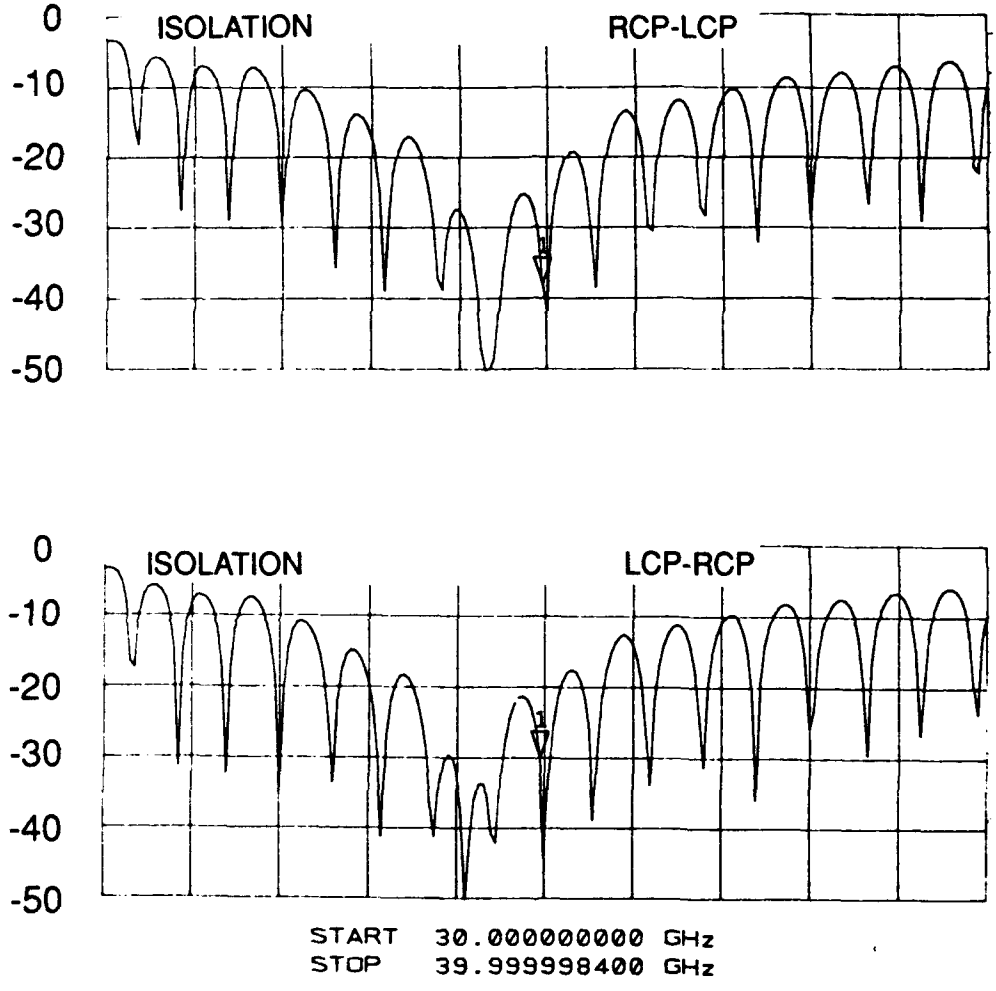

Fig. 4.2.2: The isolation of the polarizer combination 2 and 3 as a function of the frequency for circular polarization.

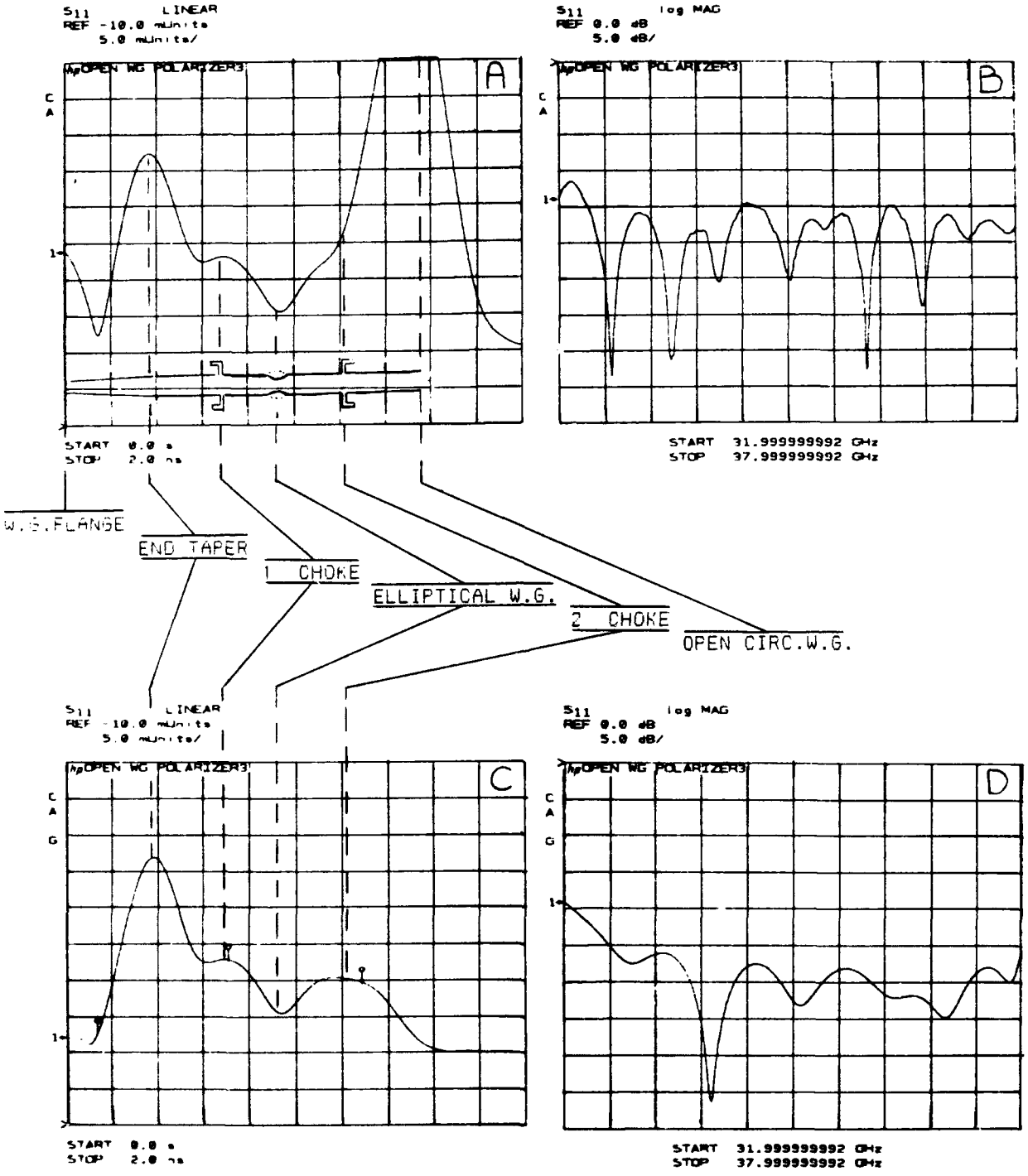

Fig. 4.2.3: Time and frequency domain measurements of polarizer 3 (A and B without gating, C and D with gating).

4.3 94.0 GHz network analyser measurements

The 94.0 GHz polarizer measurements were performed with a Wiltron 360 Network Analyser.
We first measured the time domain of the polarizer combination B and C (figure 4.3.0). The response resolution is 480 psec ≈ 15 cm.
Because the polarizer length is shorter than this resolution, the distinct scatter-centers in the polarizer can't be identified.
Polarizers B and C were connected back to back in the same way as polarizers 2 and 3 at 35.0 GHz. We used the time-gate for the return loss measurements.
The return loss of polarizer B is presented in figure 4.3.1. for linear and both circular polarizations and is better than 26 dB over 3 percent frequency bandwidth.
Figure 4.3.2 shows the insertion loss for linear and both circular polarizations. The insertion loss of the polarizer combination is 1.5 dB over a 3 percent frequency bandwidth.
In figure 4.3.3 the isolation for both circular polarizations is given. The isolation is more than 20 dB over 3 percent frequency bandwidth.

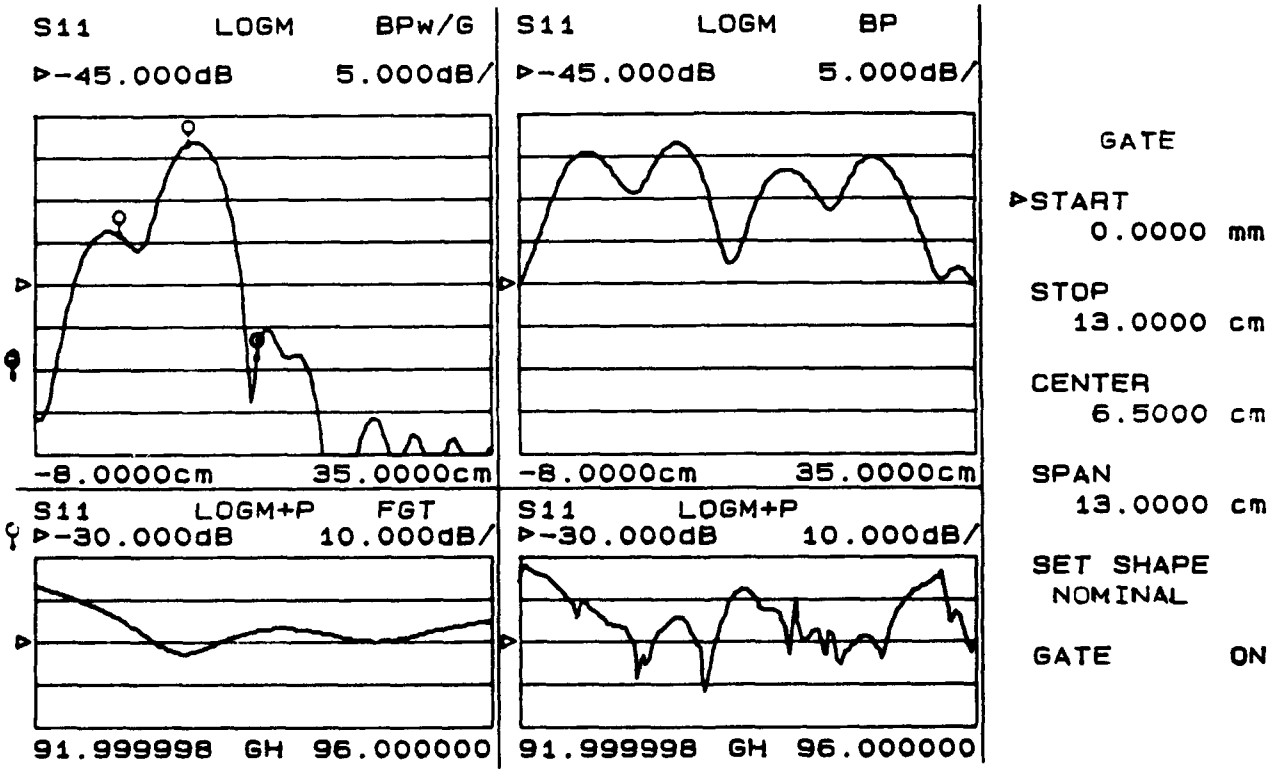

Fig. 4.3.0: Time and frequency domain measurements of the polarizer combination B and C.

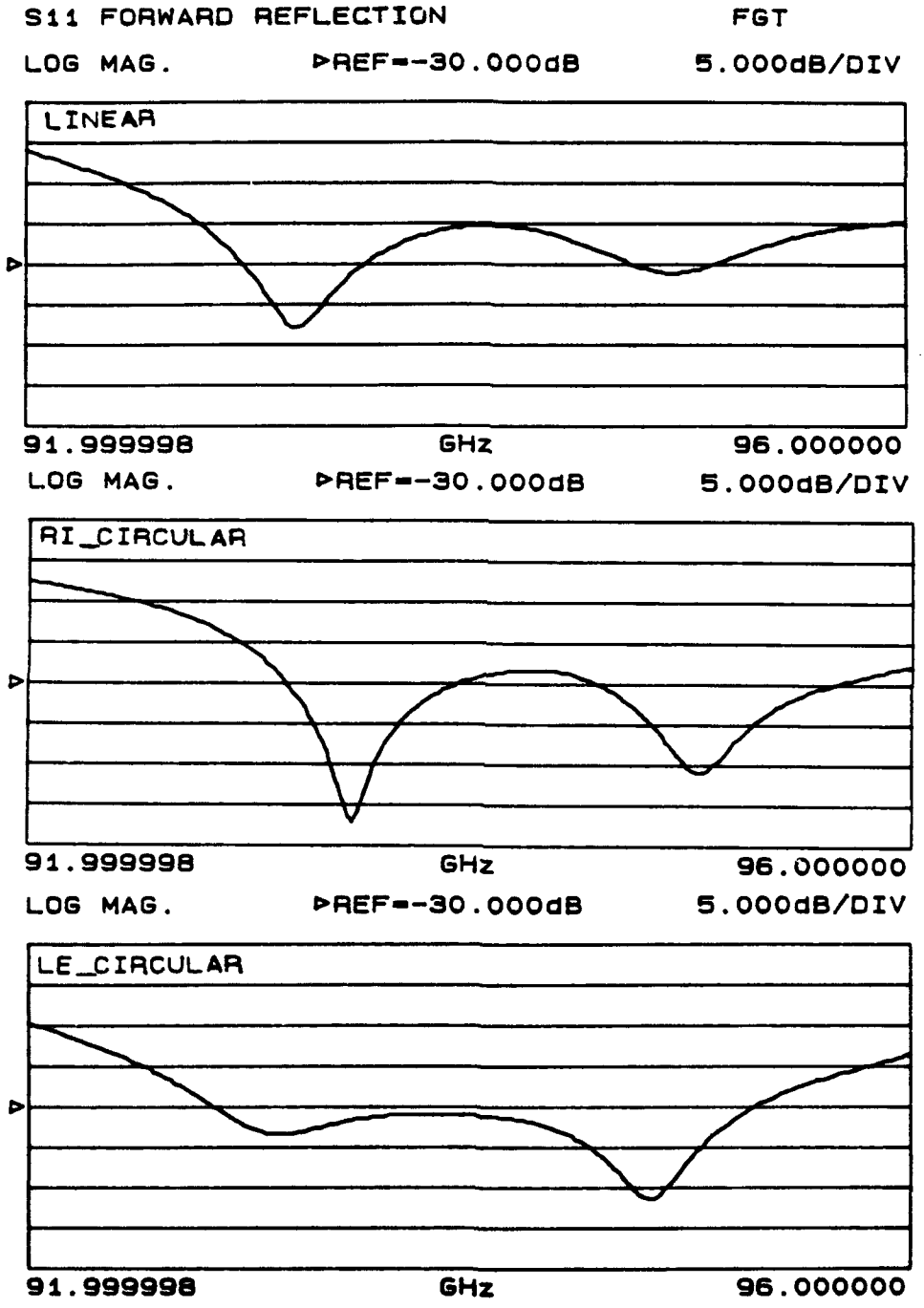

Fig. 4.3.1: The return loss of polarizer B as a function of frequency for linear, right-hand circular and left-hand circular polarization.

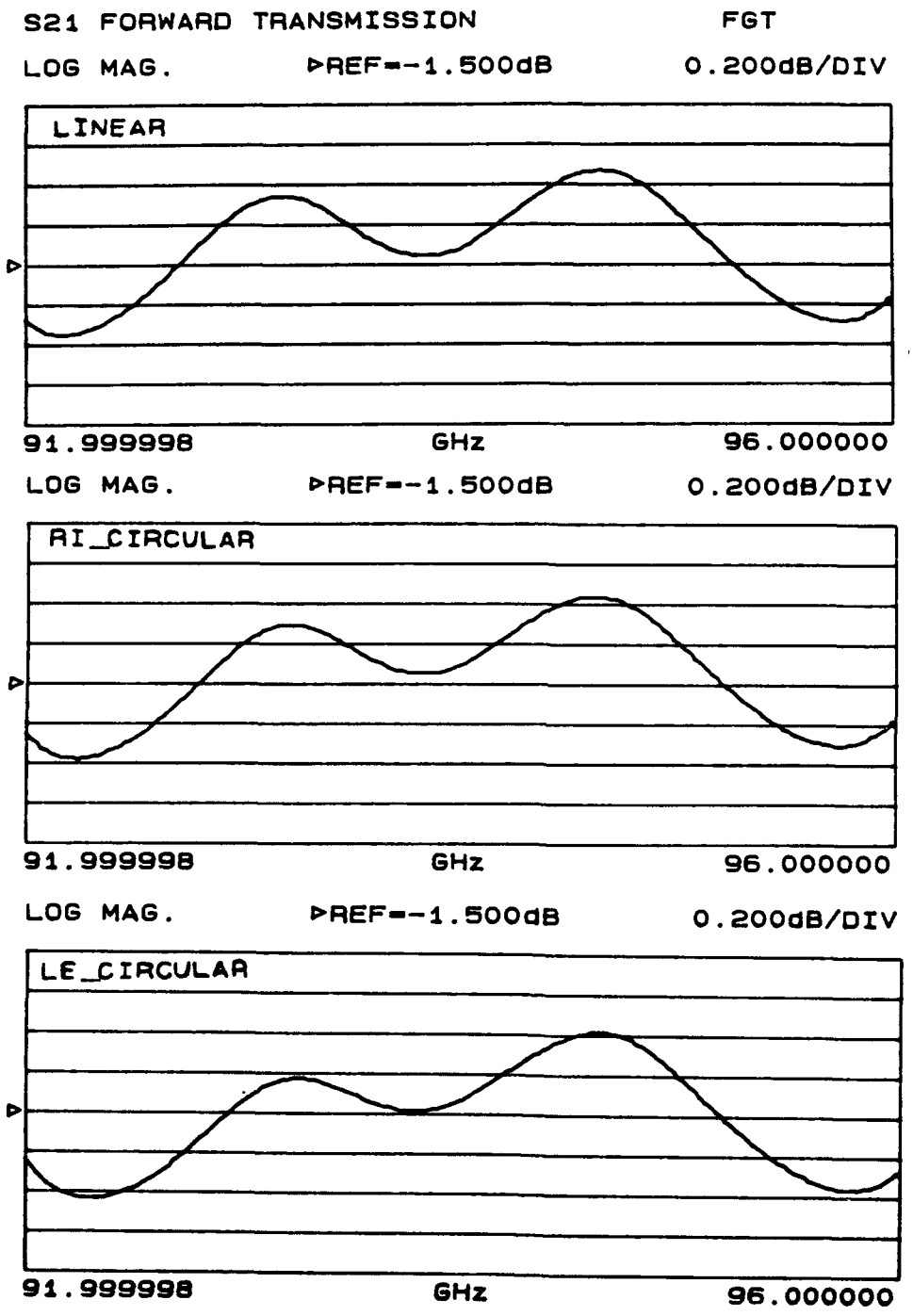

Fig. 4.3.2: The insertion loss of the polarizer-combination B and C as a function of the frequency for linear, right-hand circular and left-hand circular polarization.

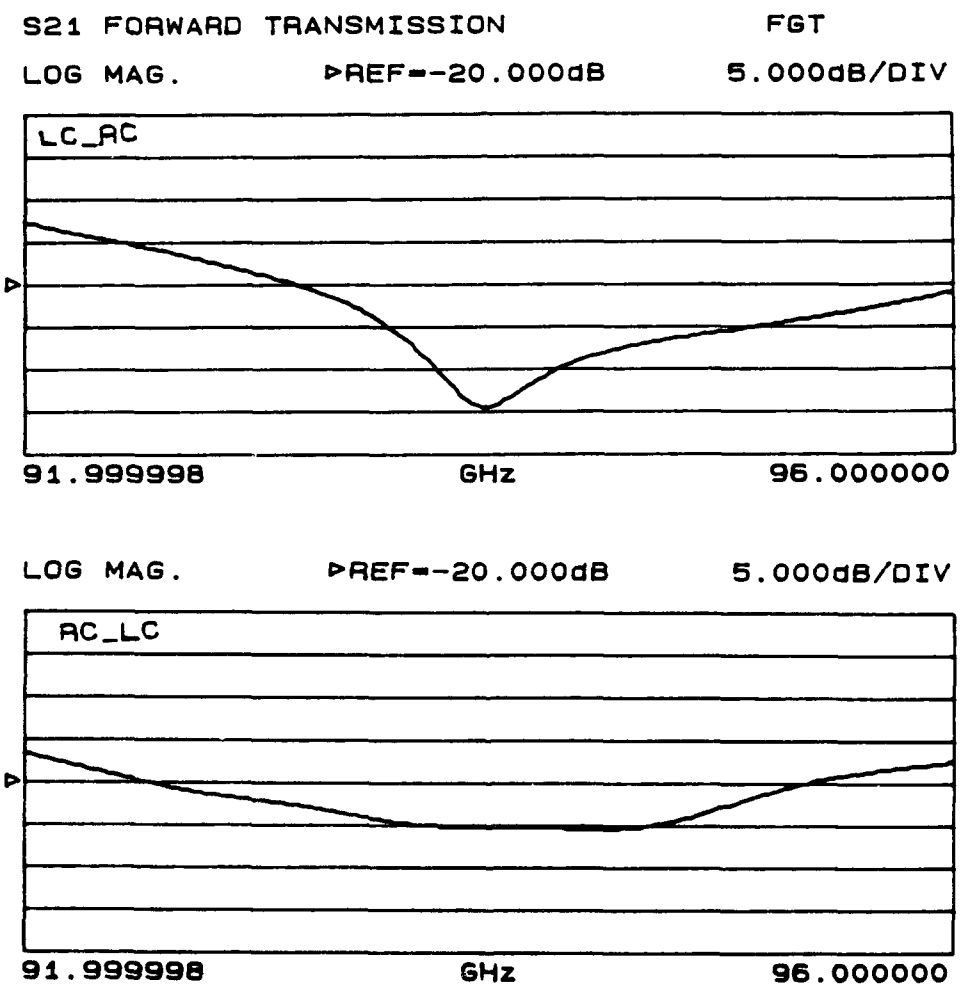

Fig. 4.3.3: The isolation of the polarizer-combination B and C as a function of the frequency for circular polarization.

5.0 CONCLUSIONS

4 High power polarizers have been realized: 2 at 35.0 GHz and 2 at 94.0 GHz.

These polarizers make use of an elliptical waveguide to convert the linearly polarized incident wave into a left-hand or right-hand circularly polarized wave. To achieve this conversion it is essential to create a 90° phase shift between the orthogonal components of the linearly polarized incident wave.

Manufacturing large numbers of these polarizers can be done, but great precision is required. Reducing the narrow inside elliptical waveguide- radius 130 μm at 94.0 GHz or 380 μm at 35.0 GHz gives a 90° phase shift. Reducing an extra 113 μm at 94.0 GHz or 255 μm at 35.0 GHz gives a 270° phase shift.

When the phase shift is 270° instead of 90° the result will be;

- an opposite circular polarization;
- a decrease of maximum power (30 percent);
- an increase of the cut-off frequency (10 percent).

The 35.0 GHz polarizer has the following properties;

- axial ratio is less than 1 dB over 5 percent bandwidth.
- return loss is better than 21 dB over 30 percent bandwidth.
- insertion loss is less than 0.3 dB over 30 percent bandwidth.
- isolation is more than 18 dB over 5 percent bandwidth.
- maximum peak power is 63 kW (11 dB better than 'quarter-wave plate' polarizers).

The 94.0 GHz polarizer has the following properties;

- axial ratio is less than 1 dB over 5 percent bandwidth.
- return loss is better than 26 dB over 3 percent bandwidth.
- insertion loss is less than 0.75 dB over 3 percent bandwidth.
- isolation is more than 20 dB over 3 percent bandwidth.
- maximum peak power is 9.5 kW (9.8 dB better than 'quarter-wave plate' polarizers).

6.0 NOMENCLATURE

a_0, a_1, a_2, a_3, a_4	Inside radius of circular waveguide
b_0	Choke radius
d	Inside diameter of circular waveguide
e	Eccentricity of the boundary ellipse
E_1, E_2	Amplitudes of field vector
E, e_θ, e_ϕ	Electrical field vectors
f_c	Centre frequency
f_{cu}	Cut-off frequency
L_c	Choke depth
L_t and L_e	Length of waveguide
Pmax	Maximum power in the circular waveguide
2q	Focal distance
s	Circumference
t	Time
v_p, v_θ, v_ϕ	Phase velocity
VSWR	Voltage Standing Wave Ratio
x, y	Rectangular coordinates
α	Angle of taper
η	Coordinate of the confocal hyperbola
λ_0	Free space wavelength
λ_c	Cut-off wavelength
λ_g	Waveguide wavelength
ξ	Coordinate of the confocal ellipse
τ	Angle between field vectors
Ψ_e, Ψ_p, Ψ_t, Ψ_2, Ψ_4	Phase shift
ω	Radial frequency

7.0 BIBLIOGRAPHY

[1] Bazzy, W.
The Microwave Engineers Handbook
Horizon House-Microwave Inc., 1966

[2] Beyer, O et al
Kleine Enzyklopadie Mathematik
VEB Bilbliographisches Institut Leibzig, 1986

[3] Harvey, A.F.
Microwave Engineering
Academic Press London & New York, 1963

[4] Lance, A.L.
Introduction to microwave theory and measurements
Mc Graw Hill Book Company Inc., 1964

[5] Marcuvitz, N.
Waveguide Handbook
Mc Graw Hill Book Company Inc., 1951

[6] Vector Measurements of high Frequency Networks
Hewlett-Packard, March 1987

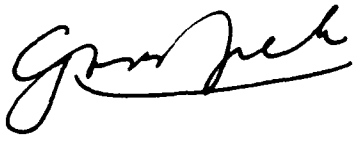

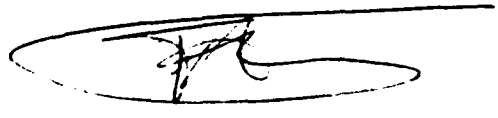

G.A. van der Spek
(group leader)

F.A. Nennie
(author)

A DERIVATION OF THE EQUATION OF THE PHASE SHIFT IN AN ELLIPTICAL WAVEGUIDE

The ellipticity of the elliptical waveguide is small and the elliptical mode-patterns of the TE_{11}-modes in an elliptical waveguide are simular to the mode-patterns of the TE_{11}-modes in a circular waveguide.
Therefore we approximated the cut-off wavelength of the elliptical waveguide with the cut-off wavelength of two circular waveguides (Appendix B).

The wavelength of the waveguide in which the circular TE_{11} mode is propagating can be calculated as follows:

$$\lambda_g = \lambda_0/\sqrt{1-(\lambda_0/\lambda_c)^2}\ [3]$$

where the cut-off wavelength $\lambda_c = 3.412a$ [3] and a is the inside radius of the circular waveguide.

So:
$$\lambda_g = \lambda_0/\sqrt{1-(\lambda_0/3.412a)^2}$$

The waveguide wavelength of the 'wide ellipse' circular waveguide is:

$$\lambda_{g2} = \lambda_0/\sqrt{1-(\lambda_0/3.412a_2)^2} \qquad \text{(A1)}$$

and of the 'narrow-ellipse' circular waveguide is:

$$\lambda_{g4} = \lambda_0/\sqrt{1-(\lambda_0/3.412a_4)^2} \qquad \text{(A2)}$$

The phase shift of the waveguide is:

$$\Psi = 360^0 L/\lambda_g\ [3] \qquad \text{(A3)}$$

where L is the waveguide length.

The phase shift of the 'wide ellipse' circular waveguide is:

$$\psi_2 = 360^0 L_e/\lambda_{g2}$$

and the phase shift of the 'narrow ellipse' circular waveguide is:

$$\psi_4 = 360^0 L_e/\lambda_{g4}$$

The phase shift of the ellipse is:

$$\psi_e = \psi_2 - \psi_4$$

Substitution in (A3) gives:

$$\psi_e = (360 L_e/\lambda_{g2}) - (360 L_e/\lambda_{g4})$$

Using (A1) and (A2):

$$\psi_e = 360 L_e \left(\frac{\sqrt{1-(\lambda_0/3.412a_2)^2} - \sqrt{1-(\lambda_0/3.412a_4)^2}}{\lambda_0} \right) \qquad \text{(A4)}$$

AN APPROXIMATION OF THE CUT-OFF FREQUENCY OF AN ELLIPTICAL WAGEGUIDE

author : H.J. Visser
institute : TNO Physics and Electronics Laboratory
date : November 1990

In figure B1 the cross-section of an elliptical waveguide is shown.
For an elliptical boundary the use of plane confocal coordinates ξ, η and z is appropriate.

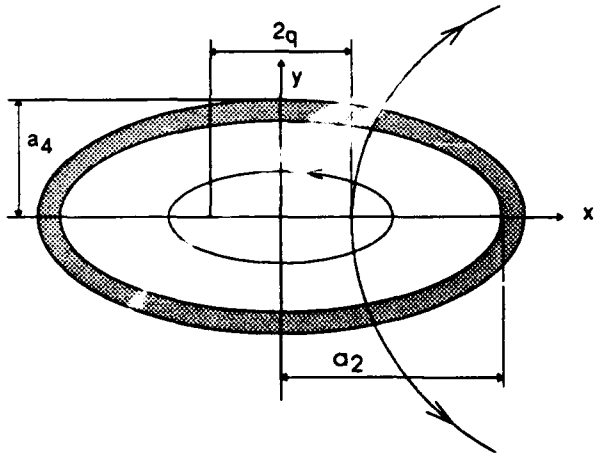

Fig. B1: The cross-section of an elliptical waveguide.

The relation between the rectangular and the elliptical coordinates are [5]:

$$x = q \cosh \xi \cos \eta \quad \text{(B1a)}$$
$$y = q \sinh \xi \sin \eta \quad \text{(B1b)}$$
$$z = z \quad \text{(B1c)}$$

The eccentricity is given by :

$$e = 1 / \cosh a \quad \text{(B2)}$$

where the boundary ellipse is defined by the coordinate $\xi = a$.

The dominant mode of an elliptical waveguide is the TE_{11}-mode [5]. Presenting a linearly polarized wave to an elliptical waveguide, of which the polarization makes an angle of 45° with the x-axis, results in propagation of even and odd TE_{11}-mode waves through the waveguide. Mode patterns of even and odd TE_{11}-modes are drawn in figure B2 and are compared with TE_{11}-patterns of a circular waveguide [5].

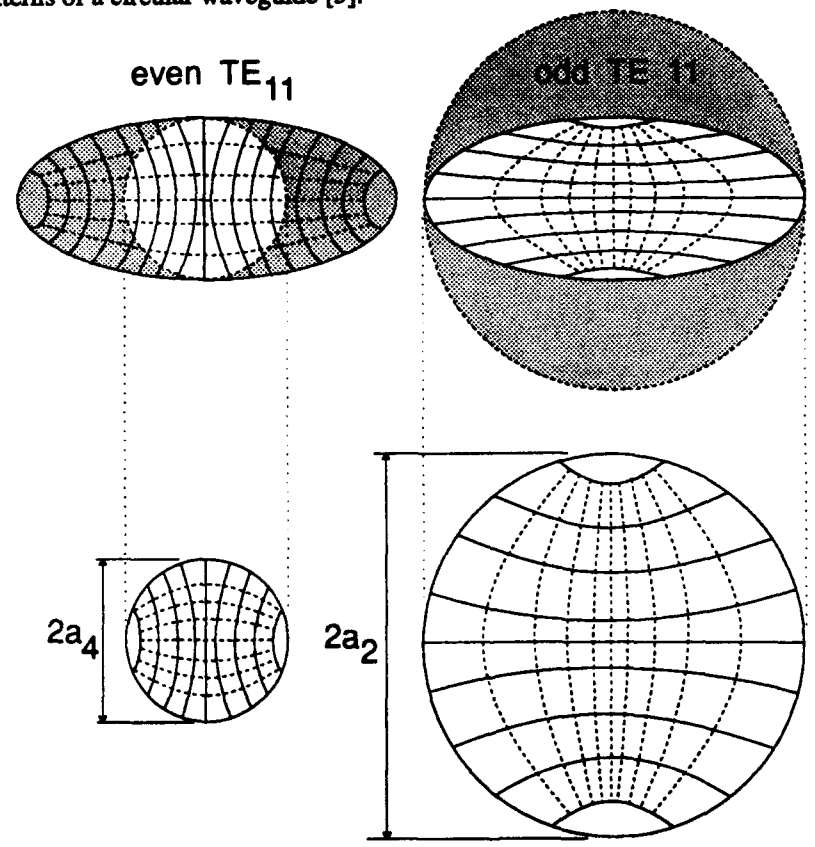

Fig. B2: Field distribution of TE_{11}-mode.

Unlike a circular waveguide, the cut-off wavelengths of an elliptical waveguide are different for even and odd modes. These elliptical mode-patterns are simular to mode-patterns of a circular waveguide with a diameter equal to the length of the elliptical E-field axes (see figure B2), it will be likely that the cut-off wavelength of even and odd modes can be approximated with the cut-off wavelength of a circular waveguide.

Because the field is concentrated along the axes, the calculation error of the cut-off wavelength will be small when the ellipticity is small.

To check this statement we compare an approximated calculation with a correct calculation of the cut-off wavelength for 4 elliptical waveguides.
To determine the cut-off wavelength of an ellitical waveguide, we used figure B3 [5].

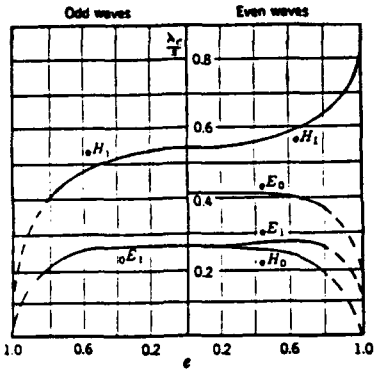

Fig. B3: Cut-off wavelengths of an elliptical waveguide.

In the determination of the cut-off wavelength, use is made of the elliptical integral formula for the circumference of the boundary ellipse.

$$s = \frac{q}{e} \int_0^{2\pi} \sqrt{1-e^2\cos^2\eta}\, d\eta, \qquad \text{(B3)}$$

as well as the constant a (see (B2)).
To obtain the constant a, the parameter representation of an ellipse is used [2]:

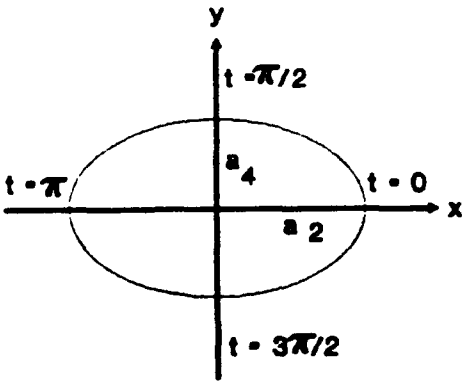

$$x = a_2 \cos t \qquad \text{(B4a)}$$
$$y = a_4 \sin t \qquad \text{(B4b)}$$

Using (B1) and with [2, p.193];

$$q = \sqrt{a_2^2 - a_4^2} \tag{B5}$$

At $t = 0$, than $x = a_2$, $\xi = a$, $\eta = 0$ and so:

$$\begin{aligned} &\sqrt{a_2^2 - a_4^2}\ \cosh(a) = a_2 \\ &\Leftrightarrow\ \cosh(a) = a_2/\sqrt{a_2^2 - a_4^2} \\ &\Leftrightarrow\ e^a + e^{-a} = 2a_2/\sqrt{a_2^2 - a_4^2} \end{aligned} \tag{B6a}$$

At $t = \pi/2$, than $y = a_4$, $\xi = a$, $\eta = \pi/2$ and so:

$$\begin{aligned} &\sqrt{a_2^2 - a_4^2}\sinh(a) = a_4 \\ &\Leftrightarrow\ \sinh(a) = a_4/\sqrt{a_2^2 - a_4^2} \\ &\Leftrightarrow\ e^a + e^{-a} = 2a_4/\sqrt{a_2^2 - a_4^2} \end{aligned} \tag{B6b}$$

Addition of (B6a) and (B6b) gives:

$$\begin{aligned} &e^a = a_2 + a_4/\sqrt{a_2^2 - a_4^2} \\ &\Leftrightarrow\ a = \ln((a_2 + a_4)/\sqrt{a_2^2 - a_4^2}) \end{aligned} \tag{B7}$$

And:

$$\cosh(a) = \frac{e^{\ln((a_2+a_4)/\sqrt{a_2^2-a_4^2})} + e^{-\ln((a_2+a_4)/\sqrt{a_2^2-a_4^2})}}{2} =$$

$$= \frac{((a_2+a_4)/\sqrt{a_2^2-a_4^2}) + (\sqrt{a_2^2-a_4^2}/(a_2+a_4))}{2} =$$

$$= a_2/\sqrt{a_2^2 - a_4^2} \tag{B8}$$

and so:

$$s = \frac{q}{e}\int_0^{2\pi}\sqrt{1-e^2\cos^2\eta}\,d\eta =$$

$$s = \frac{\sqrt{a_2^2-a_4^2}}{1/\cosh(a)}\int_0^{2\pi}\sqrt{1-[1/\cosh(a)]^2\cos^2\eta}\,d\eta =$$

$$= a_2 \int_0^{2\pi}\sqrt{1-((a_2^2-a_4^2)/a_2^2)\cos^2\eta}\,d\eta \qquad \text{(B9)}$$

The sizes of 4 elliptical waveguides and calculated values of e and s are given in table B1.

waveguide	a_2(mm)	a_4(mm)	e	s
polarizer 3	0.003345	0.00285	0.5235	0.1949
polarizer 2	0.00337	0.002805	0.5543	0.1944
polarizer c	0.00128	0.00106	0.5605	0.7368
polarizer b	0.001285	0.00105	0.5765	0.7354

Table B1: e- and s- values of elliptical waveguides.

For 4 e- values, λ_c/s has been determined with the aid of figure B3 and the cut-off wavelength have been calculated with the aid of table B1.

The cut-off wavelength of circular waveguides (approximation) have been calculated with :

$\lambda_c = 2\pi a_i/1.841$ (i=2 and 4)

The cut-off wavelength of elliptical waveguides (TE_{11}-mode) and the approximated values are tabulated in table B2.

waveguide	λ_c even TE_{11}	approxima	$\lambda_c$odd TE_{11}	approxima
polarizer 3	0.0111	0.0114	0.00965	0.00973
polarizer 2	0.0111	0.0115	0.00955	0.00957
polarizer C	0.00424	0.00437	0.00358	0.00362
polarizer B	0.00427	0.00439	0.00354	0.00358

Table B2: The cut-off wavelength of elliptical waveguides (TE_{11}-mode) and the approximated values.

Although the cut-off wavelength of the elliptical waveguides have not been calculated, but have been determined with figure B3, we can conclude that for the 4 treaded waveguides the cut-off wavelengths for even and odd TE_{11}-modes may be approximated by the cut-off wavelengths of circular waveguides with diameters equal to the lengths of the elliptical E-field axes.

REPORT DOCUMENTATION PAGE (MOD-NL)

1. DEFENSE REPORT NUMBER (MOD-NL)
TD91-3693

2. RECIPIENT'S ACCESSION NUMBER

3. PERFORMING ORGANIZATION REPORT NUMBER
FEL-91-A324

4. PROJECT/TASK/WORK UNIT NO.
20345

5. CONTRACT NUMBER
A87KL064 - A85KLU126

6. REPORT DATE
APRIL 1992

7. NUMBER OF PAGES
42 (INCL. 2 APPENDICES, EXCL. RDP + DISTRIBUTION LIST)

8. NUMBER OF REFERENCES
6

9. TYPE OF REPORT AND DATES COVERED
FINAL

10. TITLE AND SUBTITLE
HIGH POWER MILLIMETRE-WAVE POLARIZERS

11. AUTHOR(S)
F.A. NENNIE

12. PERFORMING ORGANIZATION NAME(S) AND ADDRESS(ES)
TNO PHYSICS AND ELECTRONICS LABORATORY, P.O. BOX 96864, 2509 JG THE HAGUE
OUDE WAALSDORPERWEG 63, THE HAGUE, THE NETHERLANDS

13. SPONSORING/MONITORING AGENCY NAME(S)
ROYAL NETHERLANDS ARMY AND ROYAL NETHERLANDS AIR FORCE

14. SUPPLEMENTARY NOTES

15. ABSTRACT (MAXIMUM 200 WORDS, 1044 POSITIONS)

THE OPERATION AND REALIZATION OF 4 HIGH-POWER POLARIZERS AT 35.0 GHZ AND 94.0 GHZ ARE DESCRIBED IN THIS REPORT.
RESULTS OF CALCULATIONS AND MEASUREMENTS ARE DISCUSSED.
THE REALIZED POLARIZERS MAKE USE OF AN ELLIPTICAL WAVEGUIDE TO CONVERT THE LINEARLY POLARIZED INCIDENT WAVE INTO AN OUTWARD LEFT OR RIGHT-HAND CIRCULARLY POLARIZED WAVE.
MAIN MEASUREMENT RESULTS ARE:
THE AXIAL RATIO AT 35.0 GHZ IS LESS THAN 1.0 DB OVER 5 PERCENT BANDWIDTH. THE RETURN LOSS IS BETTER THAN 21 DB (VSWR < 1.2) OVER MORE THAN 30 PERCENT BANDWIDTH. THE INSERTION LOSS IS LESS THAN 0.3 DB OVER MORE THAN 30 PERCENT BANDWIDTH. THE ISOLATION IS MORE THAN 18 DB OVER 5 PERCENT BANDWIDTH. THE MAXIMUM PEAK-POWER IS 63 KW.
THE AXIAL RATIO AT 94.0 GHZ IS LESS THAN 1.0 DB OVER 5 PERCENT BANDWIDTH. THE RETURN LOSS IS BETTER THAN 26 DB (VSWR < 1.1) OVER MORE THAN 3 PERCENT BANDWIDTH. THE INSERTION LOSS IS LESS THAN 0.75 DB OVER MORE THAN 3 PERCENT BANDWIDTH. THE ISOLATION IS MORE THAN 20 DB OVER 3 PERCENT BANDWIDTH. THE MAXIMUM PEAK-POWER IS 9.5 KW.
ALL POLARIZERS HAVE BEEN MADE WATERPROOF AND DUST-PROOF.

16. DESCRIPTORS
POLARIZATION

IDENTIFIERS
POLARIZERS
ELLIPTICAL WAVEGUIDE
CIRCULAR POLARIZED WAVE
HIGH POWER POLARIZERS

17a. SECURITY CLASSIFICATION (OF REPORT)
UNCLASSIFIED

17b. SECURITY CLASSIFICATION (OF PAGE)
UNCLASSIFIED

17c. SECURITY CLASSIFICATION (OF ABSTRACT)
UNCLASSIFIED

18. DISTRIBUTION/AVAILABILITY STATEMENT
UNLIMITED AVAILABILITY

17d. SECURITY CLASSIFICATION (OF TITLES)
UNCLASSIFIED